Dopant-modulated sound transmission with zero index acoustic metamaterials

Zhongming Gu, He Gao, Tuo Liu, Yong Li, and Jie Zhu

Citation: The Journal of the Acoustical Society of America **148**, 1636 (2020); doi: 10.1121/10.0001962
View online: https://doi.org/10.1121/10.0001962
View Table of Contents: https://asa.scitation.org/toc/jas/148/3
Published by the Acoustical Society of America

JASA ARTICLE

Dopant-modulated sound transmission with zero index acoustic metamaterials

Zhongming Gu,[1] He Gao,[1] Tuo Liu,[1] Yong Li,[2,a)] and Jie Zhu[1,b)]
[1]*The Hong Kong Polytechnic University Shenzhen Research Institute, 18 Yuexing First Avenue, Shenzhen 518057, People's Republic of China*
[2]*Institute of Acoustics, Tongji University, 1239 Siping Road, Shanghai 200092, People's Republic of China*

ABSTRACT:
Zero index metamaterials have shown the ability to achieve total transmission or reflection by embedding particular defects with various effective parameters. Here, we present that tunable sound transmission can be realized by configuring a subwavelength-sized dopant inside zero index acoustic metamaterials. Despite its small spatial signature, the dopant is able to strongly interact with the acoustic waves inside the whole zero index metamaterials. It is due to the essence of the zero effective index that can homogenize the pressure field within the metamaterials. Sound transmission can thus be fully switched on and off by adjusting the dopant's surface impedance. A simple rectangular cavity with varied lengths is proposed to provide the required impedance boundary. Our model of correlating the dopant design with sound transmission performance is validated theoretically and numerically. We further demonstrate the utilization of the proposed design to effectively modulate the sound focusing effect. Such a dopant-modulated sound transmission scheme, with its simplicity and capability, has potential applications in fields like noise control and ultrasonography. © *2020 Acoustical Society of America*. https://doi.org/10.1121/10.0001962

(Received 10 June 2020; revised 25 August 2020; accepted 27 August 2020; published online 22 September 2020)
[Editor: Badreddine Assouar] Pages: 1636–1641

I. INTRODUCTION

Zero index metamaterials (ZIM) have been studied vigorously in the scientific community owing to their intriguing properties, which are not available in nature. They have been intensively investigated in wave systems ranging from optics to acoustics.[1–14] Their near zero effective refractive indices indicate extremely large wavelengths that can effectively decouple the spatial and temporal fields, which means that waves propagating in the ZIM undergo no phase variation.[15–18] Besides, according to Snell's law, the critical angle at the interface of the ZIM declines to 0°, which only allows the vertical incident waves to pass through.[19,20] Similarly, the transmitted waves are enforced to leave the ZIM along the surface normal. Inspired by these properties, many extraordinary wave phenomena and functionalities, such as cloaking, asymmetric transmission, super coupling, antennas, and so on,[21–25] have been realized. Some recent progress demonstrated that transmission through ZIM can be modulated by doping inclusion with tailored parameters.[26,27] In this case, the transmission can be described as a function of the inclusion and its geometrical and material parameters.[2,17,18] Nguyen *et al.* and Wei *et al.* utilized the ideal material parameter model to study the transmission properties of doped ZIM in microwaves and acoustics, respectively.[2,17] However, restricted by the long wavelength approximation, artificial structures with subwavelength size often involve complex design or resonant units to acquire the predesigned material parameters.[22] Liberal *et al.* experimentally observed the high transmission within the epsilon-near-zero medium by doping a dielectric particle, but the tunable transmission still can hardly be achieved in practical realization.[26] Thus, the pursuit of modulating transmission through ZIM by a simple structure remains continuous.

To this end, we present a new insight into the transmission properties of doped ZIM. It is shown that transmitted waves passing through large size ZIM can be modulated by adjusting the boundary impedance of subwavelength dopant. For an acoustic wave, as the pressure keeps unanimous within the ZIM, wave interference at the ZIM-dopant interface can dominate the whole field. We propose a subwavelength rectangular dopant, which has one opening side and three rigid boundaries. The variable transfer impedance at the opening is done by changing the dopant depth. Our analytical model, which correlates the transmission coefficient and the transfer impedance, shows an excellent agreement with the numerical simulations using effective parameters. For full wave simulations, the air cylinders embedded in the water matrix scheme was employed among several approaches to achieve the zero refractive index.[9,22,28–30] In addition, we take the acoustic focusing as an example. By adjusting the depth of the dopant, the ZIM with a well-designed concave surface enables tunable focusing intensity. Here we only consider the impedance matched ZIM, but the conclusion can be extended to the density near zero medium similarly.[17] Such a doping strategy simplifies the

[a)]Electronic mail: yongli@tongji.edu.cn, ORCID: 0000-0001-8049-9128.
[b)]Also at: Research Center for Fluid-Structure Interactions, The Hong Kong Polytechnic University, 11 Yuk Choi Road, Hung Hom, Hong Kong SAR, People's Republic of China, ORCID: 0000-0002-2547-7775.

https://doi.org/10.1121/10.0001962

practical realization of acoustic transmission control with doped ZIM, providing new freedoms and flexibilities in the design of acoustic devices for focusing, cloaking, sensing, and so on.[31–37]

The paper is organized as follows. In Sec. II, we propose the effective medium model and validate it in numerical simulation. In Sec. III, we discuss the implementation of the impedance matched ZIM and reveal the ability of dopant in transmission modulation. In Sec. IV, modulated acoustic focusing utilizing the designed doped ZIM is presented. Section V is the conclusion.

II. THEORETICAL MODEL

For an ideal impedance matched ZIM arranged in an acoustic waveguide with width h as illustrated in Fig. 1(a), the host medium has relative refractive index $n_{r,1} = 1$ and relative impedance $Z_{r,1} = 1$, and ideal ZIM has relative refractive index $n_{r,2} = 0$ and relative impedance $Z_{r,2} = 1$. A dopant located inside the ZIM can provide impedance boundary, as marked by the red line in Fig. 1(a). The relative impedance of the dopant to the host medium at the boundary Z_R can be modulated by many schemes. In this study, we use a rectangular cavity filled with the host medium. The width and length of the cavity are a and l. Considering an incident acoustic wave $p_i = p_o e^{-ikx}$ propagating along the x axis inside the waveguide, it interacts with the ZIM and generates the reflected wave $p_r = rp_i$ and transmitted wave $p_t = tp_i$, where k is the wave number in host medium, r and t are the reflection and transmission coefficients, respectively. The acoustic pressure p_Z in the ZIM is a constant owing to the zero refractive index. Applying the pressure continuity condition on both sides of the ZIM, we have[38]

$$p_i + p_r = p_Z, \tag{1}$$

$$p_Z = p_t. \tag{2}$$

Hence, it is easy to find the underlying relation

$$t = 1 + r. \tag{3}$$

The volume flow continuity condition can be applied to the boundaries of the ZIM to solve the transmission coefficient. As neither loss nor gain has been employed in the model, the expression can be described as

$$\oint \frac{1}{2} p v_\perp dl' = 0, \tag{4}$$

where dl' denotes the contour of the ZIM and $v_\perp$ is the normal component of the particle velocity directing to the boundary of the ZIM. Since the particle velocity is forced to be zero at the rigid boundary, and the dopant embedded in the ZIM consists of one impedance boundary and three rigid boundaries, Eq. (4) can be rewritten as

$$\frac{p_i^2}{Z_{r,1}} h = \frac{p_r^2}{Z_{r,1}} h + \frac{p_t^2}{Z_{r,1}} h + \frac{p_z^2}{Z_R} a. \tag{5}$$

Then, by substituting Eq. (3) into Eq. (5), the transmission coefficient through the doped ZIM can be obtained as $t = 2/(2 + 1/Z_R a/h)$, and the power transmission takes the form

$$T = 4 \Big/ \left(2 + \frac{1}{Z_R} \frac{a}{h}\right)^2. \tag{6}$$

It can be found that when the dopant's transfer impedance Z_R is extremely large compared to that of the host medium, transmission approaches 1 regardless of the value of a/h. On the contrary, when the transfer impedance Z_R approaches 0, transmission also declines to 0 accordingly. When the value of Z_R is well between, sound transmission changes with Z_R smoothly. Here Z_R is pure acoustic reactance since neither radiation loss nor absorption in the dopant is considered.[38] Using Eq. (6), we calculate the sound transmission versus the absolute value of Z_R at different a/h. Simulation based on finite element method (FEM) and effective medium is also conducted with COMSOL Multiphysics. The effective material properties of the designed structures can be extracted from their reflection and transmission coefficients.[39–42] As shown in Fig. 1(b), the theoretical

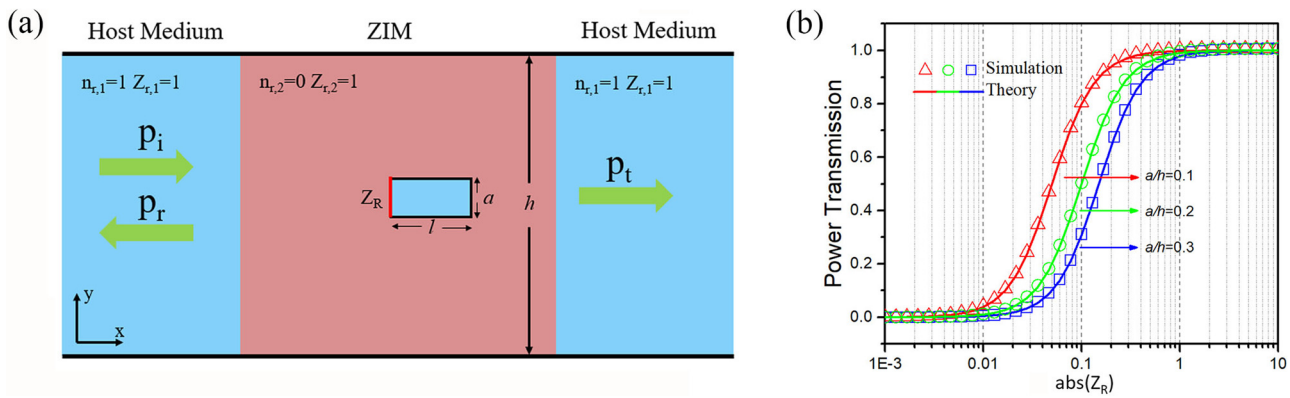

FIG. 1. (Color online) Effective medium model. (a) Zero index acoustic metamaterials inside a waveguide embedded with a rectangular dopant. The red and black lines represent the opening and hard boundaries provided by the dopant. (b) Power transmission changes with the absolute value of dopant's transfer impedance. h is fixed to be 30 cm, and a is chosen to be 10, 20, and 30 cm, respectively.

calculation agrees well with the simulation results. They clearly show the effect of doping ZIM to the sound transmission, which is decided by both the transfer impedance and the filling ratio of the dopant. For example, to totally block the incident waves with subwavelength dopant when a/h is small, the transfer impedance needs to be rather soft (get closer to 0).

The transfer impedance provided by the proposed dopant can also be modulated by changing the structure depth, which provides more possibilities that a quarter-wavelength resonator. As the dopant is surrounded by rigid walls, the transfer impedance is pure acoustic reactance and can be described as $Z_R \approx -j\rho_1 c_1 \cot(kl)$,[38] where ρ_1 and c_1 are the mass density and sound speed of the host medium, respectively. As shown in Fig. 2(a), it is obvious that the transfer impedance Z_R is 0 when $l = 0.25\lambda$ and $l = 0.75\lambda$ while reaching maximum at $l = 0.5\lambda$. Different Z_R can lead to completely different pressure field responses within the ZIM. While zero transfer impedance causes a soft boundary that forces zero pressure, an extremely large transfer impedance acts as a hard boundary so the particle velocity is close to 0. For a perfectly impedance-matched ZIM, full transmission can be guaranteed. However, with a dopant, the transmission spectrum is instead governed by its transfer impedance Z_R, as given in Fig. 2(b). Two deep transmission dips can be observed to be around $l = 0.25\lambda$ and $l = 0.75\lambda$, corresponding to the cases of zero dopant transfer impedance. The intensity fields within the doped cavity for the cases of $l = 0.25\lambda$, 0.5λ, and 0.75λ are presented in Fig. 2(b). Standing waves can be observed due to the superpositions of incident and reflected sound. The wave node can be produced at the interface of the "off" state, and the wave antinode can be produced in the "on" state. As the pressure must be consistent inside a ZIM and also continuous at the interface between the ZIM and the dopant, the signal at the dopant opening can denote the sound field inside the ZIM. In this scenario, dopant with $l = 0.5\lambda$ keeps the ZIM at "on" state with total transmission. When the depth l of dopants turns to $l = 0.25\lambda$ or 0.75λ, the ZIM will be switched to the "off" state, which prohibits any transmission. Such transmission variation with l confirms the sound transmission tunability exerted by a small structure to a large ZIM.

III. SOUND TRANSMISSION MODULATED BY DOPED ZIM

As illustrated in Fig. 3(a), the practical implementation of ZIM is realized by embedding air cylinders (density $\rho_a = 1.25\,\mathrm{kg/m^3}$ and sound speed $c_a = 343\,\mathrm{m/s}$) in water matrix (density $\rho_w = 1000\,\mathrm{kg/m^3}$ and sound speed $c_w = 1500\,\mathrm{m/s}$). The lattice constant and radius of the cylinders are $d = 10\,\mathrm{cm}$ and $R = 0.1488d$, respectively. The band structure is simulated using the eigenfrequency solver (COMSOL Multiphysics), in which two flat bands degenerate with another curved band at Γ point.[29,43] The curved band is related to the monopolar resonance, and the flat bands are related to the dipolar resonances, respectively. From the viewpoint of effective medium theory, for the degenerate modes induced by the phononic crystal system with local resonances, the effective infinite bulk modulus is associated with the monopolar resonance with well-tuned intercell coupling, while the effective zero mass density is associated with the dipolar resonance that leads to the in-phase response with the incident plane waves. Thus, this triple degeneracy corresponds to infinite effective bulk modulus and zero effective mass density simultaneously at 6758.28 Hz. Based on the effective medium approach,[39] the effective refractive index n_r and impedance Z are retrieved from the transmission and reflection properties, as presented in Figs. 3(b) and 3(c), respectively. Within the sweeping frequency range, both the real and imaginary parts of the relative refractive index approach 0 at the degenerate frequency. Meanwhile, the real part of the impedance related to that of

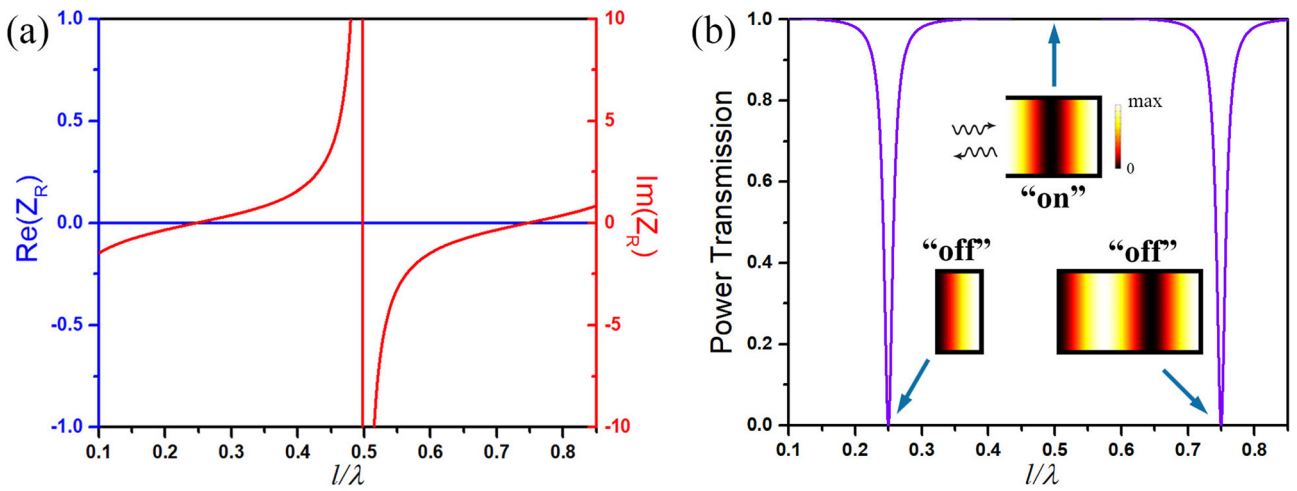

FIG. 2. (Color online) Modulation of the transfer impedance of dopant. (a) The transfer impedance versus l/λ. Two zero points happen at $l = 0.25\lambda$ and $l = 0.75\lambda$, respectively. (b) The power transmission versus l/λ. The two dips, related to the zero points of the transfer impedance, can be regarded as "off" switch; the point where the transfer impedance is mismatched compared to the host medium can be regarded as "on" switch. The insets are the sound distributions within the dopant at corresponding states.

https://doi.org/10.1121/10.0001962

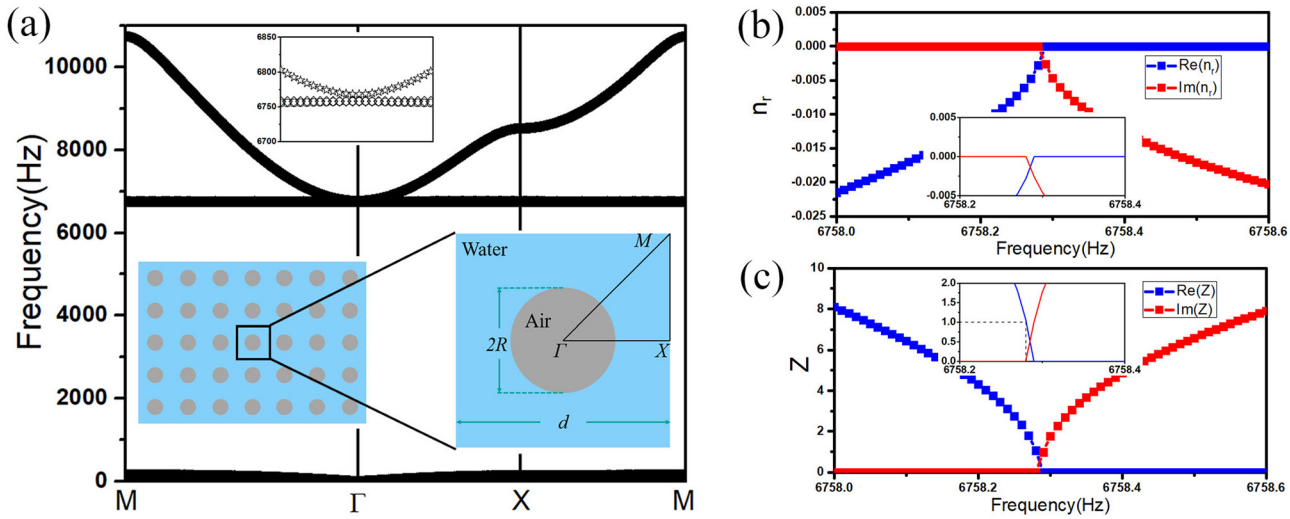

FIG. 3. (Color online) Structure of zero index acoustic metamaterial. (a) Band structure for the ZIM consisting of the air cylinders array embedded in the water. The inset is the implementation of the ZIM. The lattice constant is d, and the radius of the air cylinder $R = 0.1488d$. Two flat bands are degenerated with curved band at Γ point, associated with the Dirac-like point, signifying the existence of zero refractive index. (b) Real part (blue line) and imaginary part (red line) of the relative refractive index of the ZIM n_r versus the frequency. At the degenerate frequency, both parts are 0. (c) Real part (blue line) and imaginary part (red line) of the relative impedance of the ZIM versus the frequency. At the degenerate frequency, the real part is 1 and the imaginary part is 0.

water approaches 1 whereas its imaginary part keeps 0, giving rise to the impedance-matched full transmission.

The scenario of adding small rectangular dopant to the abovementioned ZIM is depicted in Fig. 4(a). The length and width of the dopant are set as $2d$ and d to avoid breaking the periodicity of ZIM. The vacant space enclosed by the rigid boundary can be regarded as a rigid scatterer. Although the dopant itself only occupies the space of two unit cells at most, it can efficiently determine the transmission performance of the entire ZIM, without disturbing the zero-index property. We conducted numerical simulation on a ZIM with a 5×6 array of unit cells and dopant embedded at the center. Figures 4(c) and 4(d) show the simulated pressure fields when the dopant is set to work as "on" switch and "off" switch, respectively. When the transfer impedance at the opening of the dopant is tuned to be mismatched compared to that of the host medium water, the dopant can be regarded as a hard scatterer. The incident wave will bypass it due to the extremely large effective wavelength within the ZIM. The intact wavefront and high transmission at the output side indicate the invisibility of dopant to the incident waves. Yet, when the transfer impedance drops to zero, the dopant becomes a soft scatterer that results in a vanished pressure field within the ZIM as well as a total sound reflection. By changing the depth of the dopant, the power transmission can be modulated between these two states. We calculate the transmission spectrum of the doped ZIM as a function of the dopant depth. As shown in Fig. 4(b), such an "on/off" switch mechanism is clearly supported by the split of bright band, which is associated with high transmission, and by the dark dips that are associated to the high energy reflection. Note that there is a slight difference of the position of the dip between the simulation ($l = 0.73\lambda$) and theory ($l = 0.75\lambda$), which is caused by the imperfect incident plane wave in the case of physical realization. In physical measurement, the introduction of loss may attenuate the transmission and shift the operating frequency, however, the property of zero index still can establish.[9,14,24]

IV. ACOUSTIC WAVE FOCUSING MODULATION

Acoustic wave transmission control with doped ZIM can be utilized on flexible sound focusing. For ZIM, as the transmitted waves are forced to leave along the surface normal, a concave interface at the output side will naturally provide a focused sound field. Embedding dopant, in such a case, provides a new degree of freedom targeting the sound strength at the focal point to create either weak or strong focusing effect. When the dopant's transfer impedance Z_R approaches 0, most of the incident sound energy is reflected by the ZIM, and the focusing is therefore rather weak, as demonstrated in Fig. 5(a). Conversely, when the dopant's transfer impedance Z_R is tuned to maximize the acoustic wave transmission through the ZIM, a strongly focused sound field with high intensity can be generated. It is worth mentioning that the strength of focused sound field varies in accordance with the dopant's depth. We extract acoustic wave pressure changes along the focal point area for different dopants' depths and normalize them according to the incident wave. From the plot shown in Fig. 5(c), within a small span of 0.68 to 0.74 for l/λ, the strength of the sound field around the focal point can be observed to undergo dramatic rise and fall. The ratio between the maximum and minimum amplitude at the focal can approach 2. It suggests our scheme as an effective way to tune sound focusing performance without modulating the incident signal or reshaping the concave geometry of the normal lens.

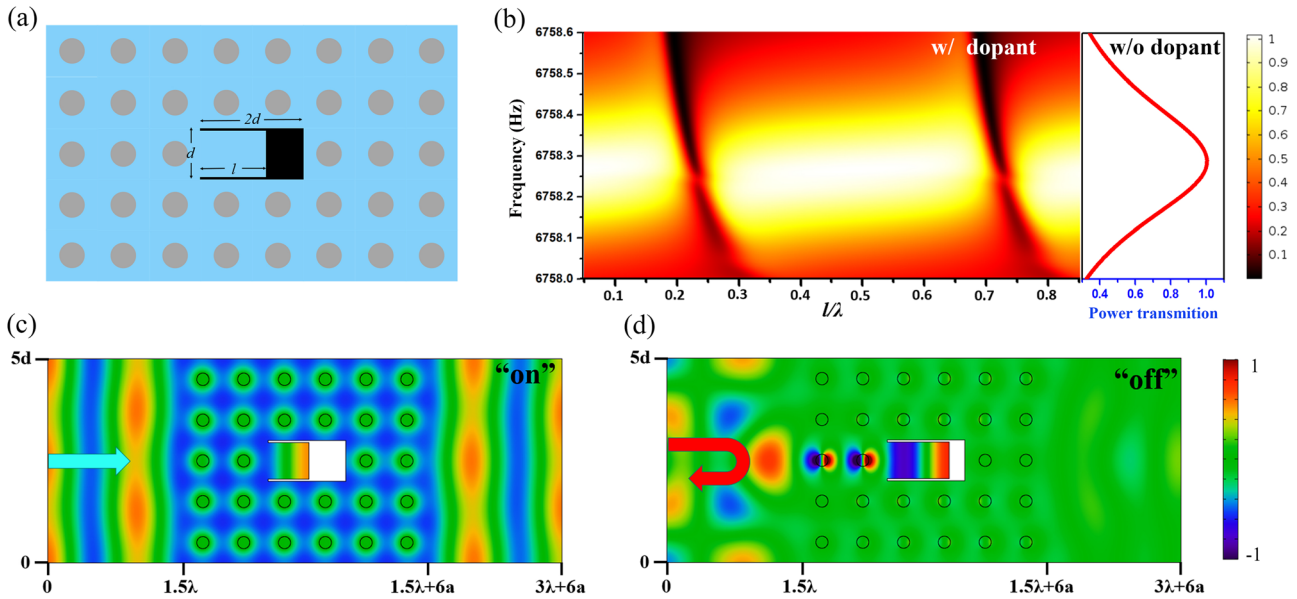

FIG. 4. (Color online) Transmission modulation. (a) Schematic diagram of the impedance matched ZIM with dopant. The dopant has length $2d$ and width d. By changing the depth of cavity l, the effective transfer impedance can be modulated at the opening. (b) Power transmission spectrum for the intact ZIM with/without dopant. (c) Numerical simulation of the acoustic pressure distribution when the dopant is set to work as "on" switch with depth $l = 0.5\lambda$. (d) Numerical simulation of the acoustic pressure distribution when the dopant is set to work as "off" switch with depth $l = 0.73\lambda$.

V. CONCLUSION

In conclusion, we have proposed and numerically demonstrated that tunable sound transmission through ZIM can be accomplished by adjusting an embedded dopant. Due to the field uniformity inside ZIM, their performance can be determined by the boundary impedance provided by dopant with a very small footprint. A 2D array of air cylinders immersed in water has been utilized to realize the impedance-matched ZIM, in which a rectangular cavity acts as the dopant. At the degenerate frequency, the sound transmission can be modulated by suitably changing the depth of the dopant, which is inconsistent with our theoretical predictions. Unlike previous approaches, our proposed doped ZIM offer an effective scheme to achieve tunable transmission without the need of structure deformation or extreme parameter distribution. A tunable sound-focusing effect is therefore demonstrated. Our study hints at the great flexibility potential of doped ZIM for complex acoustic wave modulation, which may be extended to optical and electromagnetic systems. It may open the avenue to design versatile novel devices in a variety of fields where transmission control is indispensable, such as acoustic imaging, sensing, or ultrasonic therapy.

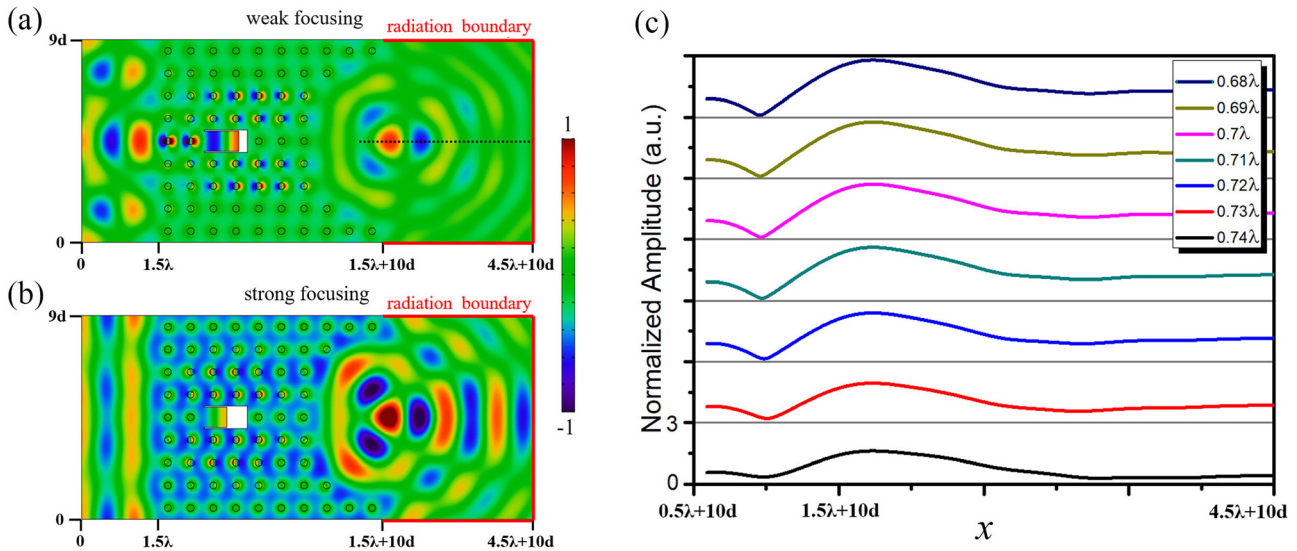

FIG. 5. (Color online) Sound focusing. (a) Simulated acoustic pressure field when the dopant is modulated to have weak sound focusing. (b) Simulated acoustic pressure field when the dopant is modulated to have strong sound focusing. (c) Acoustic pressure variation along the dashed line in (a) as a function of the dopant depth. The results are normalized to the pressure of incident wave.

https://doi.org/10.1121/10.0001962

ACKNOWLEDGMENTS

This work was supported by the National Natural Science Foundation of China (Grant Nos. 11774297 and 11704284) and the General Research Fund (GRF) scheme of Research Grants Council of Hong Kong (Grant No. PolyU 152119/18E).

[1]P. Moitra, Y. Yang, Z. Anderson, I. I. Kravchenko, D. P. Briggs, and J. Valentine, "Realization of an all dielectric zero-index optical metamaterial," Nat. Photonics **7**(10), 791–795 (2013).
[2]V. C. Nguyen, L. Chen, and K. Halterman, "Total transmission and total reflection by zero index metamaterials with defects," Phys. Rev. Lett. **105**(23), 233908 (2010).
[3]X. Huang, Y. Lai, Z. H. Hang, H. Zheng, and C. T. Chan, "Dirac cones induced by accidental degeneracy in photonic crystals and zero-refractive-index materials," Nat. Mater. **10**(8), 582–586 (2011).
[4]A. M. Mahmoud and N. Engheta, "Wave-matter interactions in epsilon-and-mu-near-zero structures," Nat. Commun. **5**, 5638 (2014).
[5]I. Liberal and N. Engheta, "Near-zero refractive index photonics," Nat. Photonics **11**(3), 149–158 (2017).
[6]F. Liu and Z. Liu, "Elastic waves scattering without conversion in metamaterials with simultaneous zero indices for longitudinal and transverse waves," Phys. Rev. Lett. **115**(17), 175502 (2015).
[7]S. A. Cummer, J. Christensen, and A. Alù, "Controlling sound with acoustic metamaterials," Nat. Rev. Mater. **1**(3), 16001 (2016).
[8]H. Ge, M. Yang, C. Ma, M.-H. Lu, Y.-F. Chen, N. Fang, and P. Sheng, "Breaking the barriers: Advances in acoustic functional materials," Natl. Sci. Rev. **5**(2), 159–182 (2018).
[9]M. Dubois, C. Shi, X. Zhu, Y. Wang, and X. Zhang, "Observation of acoustic Dirac-like cone and double zero refractive index," Nat. Commun. **8**, 14871 (2017).
[10]Y. Jing, J. Xu, and N. X. Fang, "Numerical study of a near-zero-index acoustic metamaterial," Phys. Lett. A **376**(45), 2834–2837 (2012).
[11]Z.-m. Gu, B. Liang, X.-y. Zou, J. Yang, Y. Li, J. Yang, and J.-c. Cheng, "One-way acoustic mirror based on anisotropic zero-index media," Appl. Phys. Lett. **107**(21), 213503 (2015).
[12]H. Chu, Q. Li, B. Liu, J. Luo, S. Sun, Z. H. Hang, L. Zhou, and Y. Lai, "A hybrid invisibility cloak based on integration of transparent metasurfaces and zero-index materials," Light Sci. Appl. **7**(1), 50 (2018).
[13]Z. Zhou, Y. Li, H. Li, W. Sun, I. Liberal, and N. Engheta, "Substrate-integrated photonic doping for near-zero-index devices," Nat. Commun. **10**(1), 4132 (2019).
[14]C. Xu, G. Ma, Z. G. Chen, J. Luo, J. Shi, Y. Lai, and Y. Wu, "Three-dimensional acoustic double-zero-index medium with a fourfold degenerate Dirac-like point," Phys. Rev. Lett. **124**(7), 074501 (2020).
[15]I. Liberal, Y. Li, and N. Engheta, "Reconfigurable epsilon-near-zero metasurfaces via photonic doping," Nanophotonics **7**(6), 1117–1127 (2018).
[16]R. Fleury and A. Alu, "Extraordinary sound transmission through density-near-zero ultranarrow channels," Phys. Rev. Lett. **111**(5), 055501 (2013).
[17]Q. Wei, Y. Cheng, and X.-j. Liu, "Acoustic total transmission and total reflection in zero-index metamaterials with defects," Appl. Phys. Lett. **102**(17), 174104 (2013).
[18]J. Hao, W. Yan, and M. Qiu, "Super-reflection and cloaking based on zero index metamaterial," Appl. Phys. Lett. **96**(10), 101109 (2010).
[19]C. Shen, Y. Xie, J. Li, S. A. Cummer, and Y. Jing, "Asymmetric acoustic transmission through near-zero-index and gradient-index metasurfaces," Appl. Phys. Lett. **108**(22), 223502 (2016).
[20]Y. Li, B. Liang, Z.-m. Gu, X.-y. Zou, and J.-c. Cheng, "Unidirectional acoustic transmission through a prism with near-zero refractive index," Appl. Phys. Lett. **103**(5), 053505 (2013).
[21]Y. Li, B. Liang, X.-y. Zou, and J.-c. Cheng, "Extraordinary acoustic transmission through ultrathin acoustic metamaterials by coiling up space," Appl. Phys. Lett. **103**(6), 063509 (2013).
[22]Z. Liang and J. Li, "Extreme acoustic metamaterial by coiling up space," Phys. Rev. Lett. **108**(11), 114301 (2012).
[23]Y. Fu, L. Xu, Z. Hong Hang, and H. Chen, "Unidirectional transmission using array of zero-refractive-index metamaterials," Appl. Phys. Lett. **104**(19), 193509 (2014).
[24]T. Zhang, Y. Cheng, B.-G. Yuan, J.-Z. Guo, and X.-J. Liu, "Compact transformable acoustic logic gates for broadband complex Boolean operations based on density-near-zero metamaterials," Appl. Phys. Lett. **108**(18), 183508 (2016).
[25]C. Ma, S. Gao, Y. Cheng, and X. Liu, "Acoustic metamaterial antennas for combined highly directive-sensitive detection," Appl. Phys. Lett. **115**(5), 053501 (2019).
[26]I. Liberal, A. M. Mahmoud, Y. Li, B. Edwards, and N. Engheta, "Photonic doping of epsilon-near-zero media," Science **355**(6329), 1058–1062 (2017).
[27]J. Luo, B. Liu, Z. H. Hang, and Y. Lai, "Coherent perfect absorption via photonic doping of zero-index media," Laser Photonics Rev. **12**(8), 1800001 (2018).
[28]F. Liu, X. Huang, and C. T. Chan, "Dirac cones at $\vec{k}=0$ in acoustic crystals and zero refractive index acoustic materials," Appl. Phys. Lett. **100**(7), 071911 (2012).
[29]X.-F. Zhu, "Effective zero index in locally resonant acoustic material," Phys. Lett. A **377**(31–33), 1784–1787 (2013).
[30]Y. Gu, Y. Cheng, J. S. Wang, and X. J. Liu, "Controlling sound transmission with density-near-zero acoustic membrane network," J. Appl. Phys. **118**(2), 024505 (2015).
[31]T. Liu, F. Chen, S. Liang, H. Gao, and J. Zhu, "Subwavelength sound focusing and imaging via gradient metasurface-enabled spoof surface acoustic wave modulation," Phys. Rev. Appl. **11**(3), 034061 (2019).
[32]W. Zhu, X. Fang, D. Li, Y. Sun, Y. Li, Y. Jing, and H. Chen, "Simultaneous observation of a topological edge state and exceptional point in an open and non-Hermitian acoustic system," Phys. Rev. Lett. **121**(12), 124501 (2018).
[33]H. Gao, Y. F. Zhu, X. D. Fan, B. Liang, J. Yang, and J. C. Cheng, "Non-blind acoustic invisibility by dual layers of homogeneous single-negative media," Sci. Rep. **7**, 42533 (2017).
[34]C. Shi, M. Dubois, Y. Wang, and X. Zhang, "High-speed acoustic communication by multiplexing orbital angular momentum," Proc. Natl. Acad. Sci. U.S.A. **114**(28), 7250–7253 (2017).
[35]Y. Chen, H. Liu, M. Reilly, H. Bae, and M. Yu, "Enhanced acoustic sensing through wave compression and pressure amplification in anisotropic metamaterials," Nat. Commun. **5**, 5247 (2014).
[36]H. Gao, X. Fang, Z. Gu, T. Liu, S. Liang, Y. Li, and J. Zhu, "Conformally mapped multifunctional acoustic metamaterial lens for spectral sound guiding and Talbot effect," Research **2019**, 1748537.
[37]Y. Cheng, C. Zhou, B. G. Yuan, D. J. Wu, Q. Wei, and X. J. Liu, "Ultra-sparse metasurface for high reflection of low-frequency sound based on artificial Mie resonances," Nat. Mater. **14**(10), 1013–1019 (2015).
[38]P. M. Morse, *Theoretical Acoustics*, edited by K. U. Ingard (McGraw-Hill, New York, 1968).
[39]V. Fokin, M. Ambati, C. Sun, and X. Zhang, "Method for retrieving effective properties of locally resonant acoustic metamaterials," Phys. Rev. B **76**(14), 144302 (2007).
[40]D. Torrent and J. Sánchez-Dehesa, "Effective parameters of clusters of cylinders embedded in a nonviscous fluid or gas," Phys. Rev. B **74**(22), 224305 (2006).
[41]D. Torrent and J. Sánchez-Dehesa, "Acoustic metamaterials for new two-dimensional sonic devices," New J. Phys. **9**(9), 323 (2007).
[42]M. Yang, G. Ma, Y. Wu, Z. Yang, and P. Sheng, "Homogenization scheme for acoustic metamaterials," Phys. Rev. B **89**(6), 064309 (2014).
[43]Y. Li, Y. Wu, and J. Mei, "Double Dirac cones in phononic crystals," Appl. Phys. Lett. **105**(1), 014107 (2014).